Neutron Diffraction Study of Multiferroic $0.6NiFe_2O_4/0.4BaTiO_3$ Composite

Engkir Sukirman, Yosef Sarwanto, Syahfandi Ahda, and Andon Insani

Centre for Science and Technology of Advance Materials-BATAN, Puspiptek, Serpong 15314, Indonesia

*e-mail: engkirs@gmail.com

Abstract

Neutron diffraction study on the $0.6NiFe_2O_4/0.4BaTiO_3$ multiferroic composite has been carried out. The $0.6NiFe_2O_4/0.4BaTiO_3$ multiferroic composites have been synthesized by solid reaction method. In this study, 20 g of $BaTiO_3$ (BTO) and 20 g of $NiFe_2O_4$ (NFO) compounds were prepared from the powder raw materials of BaO_3 and TiO_2 for BTO, and NiO and Fe_2O_3 for NFO. Furthermore, both BTO and NFO were each crushed for 5 hours using High Energy Milling (HEM). Then the BTO and NFO were calcined in the furnace at 950 °C/5 hours and 900 °C/5 hours, respectively. Both NFO and BTO precursors were manually mixed with a weight percent ratio of NFO:BTO was 100:0, 60:40, and 0:100, hereinafter referred to NFO, NFO/BTO, and BTO, respectively. Then the three samples were pressed into pellets. The pellets were then sintered at 1150 °C/5 hours with a heating rate of about 44.8 °C/min. Once cooled to room temperature within the furnace it was obtained NFO, BTO, and NFO/BTO multiferroic composite. The magnetic properties of the material were observed with the aid of the Vibrating Sample Magnetometer (VSM) instrument. The nuclear structure of BTO, and the magnetic structure of NFO, and NFO/BTO multiferroic composite were determined by neutron diffraction technique using the high resolution powder neutron diffractometer. The cations arrangement of NFO was obtained by whole pattern fitting with the Rietveld method based on neutron diffraction data using FullProf software. The cations arrangement was obtained by refining the occupancy of individual cation at tetrahedral and octahedral sites. The results of the analysis show that both NFO and 0.6NFO/0.4BTO samples have a mixed spinel structure, it means that there are cations of Ni^{2+} and Fe^{3+} on A-site and B-site. In NFO sample, the cations distribution among the A-site and B-site of $NiFe_2O_4$ is $[Ni_{0.002}Fe_{0.852}][Ni_{0.006}Fe_{0.862}]_2O_4$. The cations distribution among the A-site and B-site of $NiFe_2O_4$ in 0.6NFO/0.4BTO samples is $[Ni_{0.0250}Fe_{0.8975}] [Ni_{0.012}Fe_{0.950}]_2O_4$. So, the effect of adding BTO as a composite is to increase Ni^{2+} occupancy by 12.5 times on A-site and 2 times on B-site. The magnetic moment of multiferroic 0.6NFO/0.4BTO composite is 2.4(5) μ_B same as one of NFO. The BTO content in the composite has caused tensile strains induced into the NFO lattice, and at the same time, tensile strains of NFO caused the compressive strain on the *c* lattice of BTO even though the unit cell volume of BTO is also increasing from 64.100(5) to 64.374(6) $Å^3$.

Abstract

Studi Difraksi Neutron pada Komposit *Multiferroic* 0,6NiFe₂O₄/0,4BaTiO₃. Telah dilakukan studi difraksi neutron pada komposit *multiferroic* $0,6NiFe_2O_4/0,4BaTiO_3$. Komposit *multiferroic* $0,6NiFe_2O_4/ 0.4BaTiO_3$ disintesis dengan metode reaksi padat. Dalam studi ini, 20 g senyawa $BaTiO_3$ (BTO) dan 20 g $NiFe_2O_4$ (NFO) dibuat dari bahan baku bubuk BaO_3 dan TiO_2 untuk BTO, dan NiO dan Fe_2O_3 untuk NFO. Selanjutnya, BTO dan NFO masing-masing digerus selama 5 jam menggunakan *High Energy Milling* (*HEM*). Kemudian BTO dan NFO dikalsinasi dalam tungku masing-masing pada 950 °C/5 jam dan 900 °C/5 jam. Prekursor NFO dan BTO dicampurkan secara manual dengan perbandingan persen berat NFO:BTO adalah 100:0, 60:40, dan 0:100, selanjutnya disebut berturut-turut NFO, NFO/BTO, dan BTO. Kemudian ketiga cuplikan itu masing-masing ditekan menjadi pelet. Pelet selanjutnya disinter pada 1150 °C/5 jam dengan laju pemanasan sekitar 44,8 °C/menit. Setelah didinginkan hingga suhu kamar dalam tungku, maka diperoleh NFO, BTO, dan komposit *multiferroic* NFO/BTO. Sifat magnetik material diamati dengan bantuan instrumen *Vibrating Sample Magnetometer* (*VSM*). Struktur nuklir BTO, dan struktur magnetik NFO, dan komposit *multiferroic* NFO/BTO ditentukan dengan teknik difraksi neutron menggunakan difraktometer neutron serbuk resolusi tinggi. Distribusi kation NFO diperoleh dengan metode analisis Rietveld menggunakan perangkat lunak FullProf berdasarkan data difraksi neutron. Analisis data dilakukan dengan melakukan penghalusan faktor hunian kation-kation di *situs* tetrahedral dan oktahedral. Hasil analisis menunjukkan bahwa cuplikan NFO dan 0,6NFO/0,4BTO memiliki struktur *spinel* tercampur, itu berarti ada kation Ni^{2+} dan Fe^{3+} baik pada situs-A maupun situs-B. Dalam cuplikan NFO, distribusi kation pada situs-A dan situs-B fasa $NiFe_2O_4$ adalah $[Ni_{0,002}Fe_{0,852}] [Ni_{0,006}Fe_{0,862}]_2$. Distribusi kation pada situ-A dan situs-B fasa $NiFe_2O_4$ dalam cuplikan 0,6NFO/0,4BTO adalah $[Ni_{0,0250}Fe_{0,8975}] [Ni_{0,012}Fe_{0,950}]_2$. Jadi, efek penambahan BTO sebagai komposit

adalah meningkatkan hunian Ni^{2+} sebesar 12,5 kali di situs-A dan 2 kali pada situs-B. Momen magnetik komposit 0,6NFO/0,4BTO *multiferroic* adalah 2,4 (5) μ_B sama dengan momen magnetik pada NFO. Kandungan BTO dalam komposit telah menyebabkan regangan tarik yang diinduksikan ke dalam kisi NFO, dan pada saat yang sama, regangan tarik NFO menyebabkan regangan tekan pada kisi BTO walaupun volume sel satuan BTO juga meningkat dari 64,100(5) hingga 64,374(6) $Å^3$.

Keywords: synthesis, characterization, multiferroic, nickel ferrite, barium titanate, neutron diffraction

1. Introduction

Multiferroic composite materials consisting both magnetic and ferroelectric phase are of great interests. This is because of the existence magnetoelectric (ME) coupling property may lead to novel RF devices. However, only a few single phase materials have these multifunctional properties in nature. In addition, these intriguing multiferroic properties in a single phase are observed only in a few systems, and the magnetoelectric coupling usually occurs under extreme conditions, such as very high magnetic fields and/or very low temperatures, because the ferroelectric and magnetic orders have opposite requirements to the 3d-orbital occupancy [1]. An alternative method for obtaining multiferroic materials is to fabricate multilayer composites [2]. The multiferroic composites consisting of ferroelectric, such as $BaTiO_3$ (BTO) and ferromagnetic materials, such as spinel ferrite of $NiFe_2O_4$ (NFO) which is then written as NFO/BTO multiferroic composite. These composites have high potential for applications. It can be used in a wide range of applications as extremely sensitive ac magnetic field sensors [3], electric-field-controlled magnetic memories [4], and tunable microwave devices [5]. Compared to conventional tunable microwave magnetic devices that are tuned by magnetic field, these dual *H*- and *E*-field tunable microwave multiferroic devices are much more energy efficient, compact, and light-weight [6].

Spinel ferrites are the soft ferrimagnets having the general formula AB_2O_4 with two inequivalent cation lattice sites tetrahedral (A-site) and octahedral (B-site), where A is divalent cation (Fe^{2+}, Mn^{2+}, Co^{2+}, Ni^{2+}, Zn^{2+}, Sr^{2+}, Bi^{2+}, etc.) and B is trivalent cation (Fe^{3+}). In normal spinel structure, tetrahedral site is occupied by divalent cation, and octahedral site is occupied by trivalent cation. In inverse spinel configuration, tetrahedral site is fully occupied by half of trivalent atom (Fe^{3+}) and other half of trivalent atom (Fe^{3+}), and all divalent atom occupy the octahedral site [7].

The importance of neutron diffraction techniques is to obtain an understanding of magnetic structure of the NFO/BTO multiferroic composite. X-ray diffraction study has been done before on the sample of (100-x) $BaTiO_3$/x$NiFe_2O_4$ which has been prepared via a two steps standard solid-state reaction method [7]. It was observed in this study that the magnetic structure of NFO in 0.6NFO/0.4BTO composite crystallized into a mixed spinel structure with the cation arrangement of $[Ni_{0.88}Fe_{1.12}][Ni_{0.12}Fe_{0.88}]_2O_4$. The Ni^{2+} and Fe^{3+} cationic occupancy factors are written without mentioning the number of accuracy, also the occupancy factor at A-site is greater than 1.0. Whereas in the study by means of neutron diffraction [8], the Ni^{2+} and Fe^{3+} cations occupy about 30% and 70% of places at the A-site. This means that the occupancy factor at A-site is not greater than 1.0. The aim of the present paper is to clarify the crystal and magnetic structure of the 0.6NFO/0.4BTO multiferroic composite by means of neutron diffraction using the high resolution powder diffractometer.

2. Experimental Procedure

In this research we have prepared the compounds of $BaTiO_3$ (BTO) and $NiFe_2O_4$ (NFO). BTO was made from the oxide materials of $BaCO_3$ and TiO_2 in powder form, while the NFO was synthesized from NiO and Fe_2O_3 powders. The raw materials were each weighed by an appropriate mole ratio, i.e. Ba:Ti= 1:1 and Ni:Fe = 1:1. The raw materials of $BaTiO_3$ and $NiFe_2O_3$ were each inserted into a vial made of stainless steel, into each vial then were inserted 5 pieces of steel balls, where the weight of 1 steel balls is about 2 g. Next milling for 5 hours, then crushed manually for about 15 minutes with mortar agate.

Then the precursors were calcined in the furnace at 950 °C/5 hours and 900 °C/5 hours for the BTO and NFO, respectively [9]. The calcination were done three times and after calcination, the precursor was crushed manually for 15 minutes. Both types of NFO and BTO precursors were mixed together with a weight percent ratio of NFO: BTO is 100:0, 60:40, and 0:100, hereafter referred to NFO, NFO/BTO, and BTO, respectively (Table 1).

Table 1. The Weight Percent of BTO and NFO to be Made Into Composites of NFO/BTO

Sample	Weight % of BTO	Weight % of NFO
NFO	0	100
NFO/BTO	40	60
BTO	100	0

The three precursors were separated into two parts, where the weight of each precursor is 3.5 g, then inserted into the dyes, pressed at a pressure of 3,000 psi for 90 seconds, obtained ten pellets of precursor. The pellets were then loaded on an alumina boat, inserted into the furnace, sintered at 1150 °C/5 hours with a heating rate of about 44.8 °C/min. After cooling to room temperature in the furnace, the sample of 0.6NFO/0.4BTO multiferroic composite was obtained together with NFO and BTO samples.

The next step was the sample characterization. Since the characterization is usually performed on the sample of powder form, the pellets were crushed manually using a mortar agate in such a way that it became a smooth powder. The neutron powder diffraction experiments were undertaken with the high-resolution powder diffractometer (HRPD), λ=1.8220Å at the Neutron Beams Technology Laboratory of BATAN, Serpong, Indonesia. The samples were loaded in a cylindrical vanadium holder. The data were collected in the scattering angular range of 2.5º up to 157º in the interval of 0.05º for room temperature measurements. The exact detector positions, which were not always 0.05º, were confirmed by the electronic encoder. The data reduction, including the detector efficiency correction, was performed after the measurements. The neutron diffraction data was refined
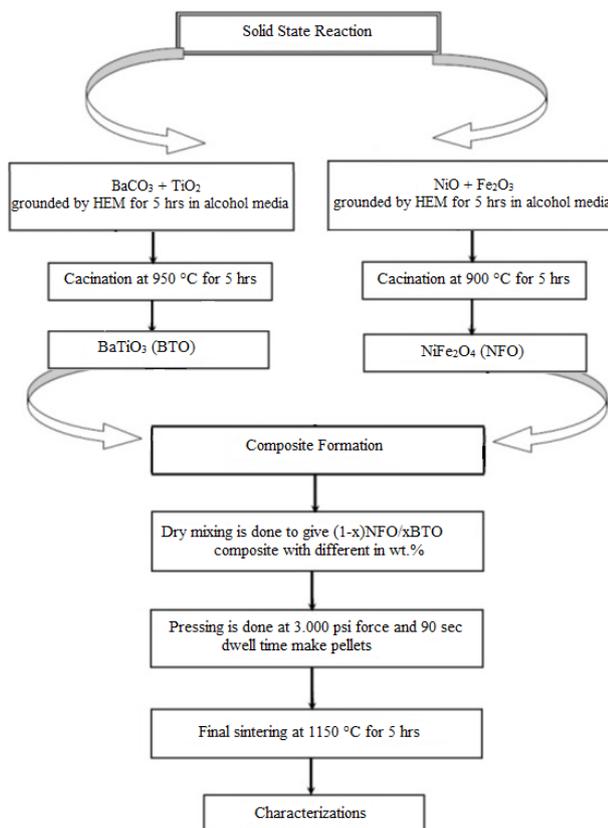

Figure 1. The Flow Chart for Synthesis Process of the 0.6NFO/0.4BTO Multiferroic Composite

using FullProf software [10]. The magnetic properties of materials were characterized using VSM (Vibrating Sample Magnetometer) Oxford Type1.2 Hin method at PSTBM, BATAN Serpong. Measurement of magnetic properties of materials was made in an applied magnetic field to a maximum value of 1 Tesla. VSM measurements was carried out at room temperature. The flow chart for synthesis process of the 0.6NFO/0.4BTO multiferroic composite is shown in Figure 1.

3. Results and Discussion

The characterization of NFO, BTO and 0.6NFO/0.4BTO samples was carried out using the neutron diffraction method, by utilizing the high-resolution neutron powder diffractometer. Neutron diffraction data were analyzed by Rietveld method using FullProf software [10] by assuming the *Fd-3m* space group for NFO sample and the *P4mm* space group for BTO sample. Peak profiles were fitted using Thompson-Cox-Hastings pseudo-Voigt*Axial divergence asymmetry function with the background mode: 6-coefficients polynomial function. The reliability index of neutron diffraction patterns analysis depends on the goodness of fit (GOF) parameter, which is stated by χ^2, where the smaller the value, the better is the quality of the fittings.

The first step is analysis of the nuclear structure of NFO, hereinafter referred to as (NFO)$_N$. The result shows that all of the diffraction peaks coincide with the calculation results based on the nuclear peaks (Figure 2). This means that the nuclear peaks coincide with the magnetic peaks. There are no additional peaks due to scattering from the magnetic phase. So the magnetic structure would have a propagation vector k = (0,0,0). As the propagation vector is k = (0,0,0), the magnetic unit cell is identical to the nuclear cell. Thus, in the spinel type structure, magnetic unit cell is the same as the crystallographic unit cell with identical symmetry relations. Therefore, the magnetic Bragg peaks superimpose the nuclear Bragg peaks, giving rise to an additional intensity [11]. The dots are the observed intensity, the solid line is the calculated intensity, and the difference pattern is shown at the bottom of the chart. The upper short vertical line show Bragg peak positions for the nuclear phase.

Analysis of the magnetic structure of NFO which is identified as (NFO)$_M$ is carried out with the two-phase input, namely nuclear, and magnetic phase of $NiFe_2O_4$, and the Rietveld refinement is carried out by trial and error. The first assumption, is that the cations of Ni^{2+} is arranged as to occupy the A-site predominantly. The second assumption, it is the Fe^{3+} cations which predominantly occupy the A-site. Next, the refinement is carried out to determine which data will give the smallest χ^2.

The analysis is based on the first and second assumptions giving χ^2 of 2.1 and 1.9, respectively. So, the second assumption is the most appropriate arrangement, and the diffraction pattern of the analysis based on the second assumption is shown in Figure 3. The dots are the observed intensity, the solid line is the calculated intensity, and the difference pattern is shown at the bottom of the chart. The upper short vertical lines show Bragg positions for the nuclear phase. The second short vertical lines show Bragg peak positions for the magnetic phase. The neutron diffraction patterns of the NFO sample shows sharp peaks. No impurity phases are observed within the detected limits of high resolution neutron diffraction.
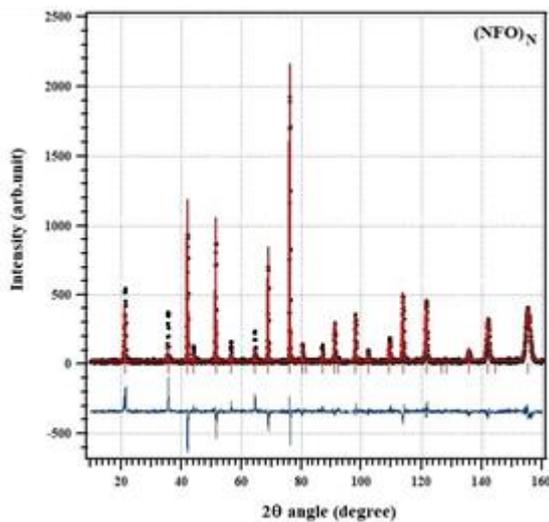

Figure 2. Rietveld Refinement Results of NiFe$_2$O$_4$ (NFO) Based on Nuclear Phase which is Identified as (NFO)$_N$
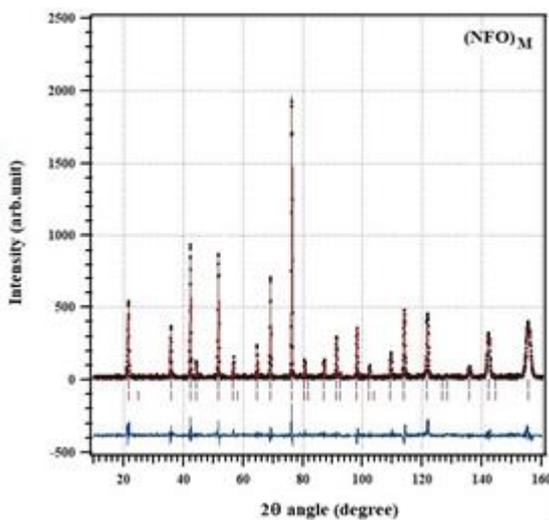

Figure 3. Rietveld Refinement Results of NiFe$_2$O$_4$ (NFO) Based on Nuclear-, and Magnetic Phase which is Identified as (NFO)$_M$

The Rietveld refinement results of atomic coordinate fractions (x_j, y_j, z_j), and occupation factors (g_j), lattice parameters (a, b, c), magnetic moments (μ_A, μ_B), weight percents (W_t), and average crystallite size (D_{av}) are shown in Table 2. The number in parentheses is the standard deviation that is imposed on the last number after the decimal point. The lattice parameter of (NFO)$_M$ is $a = 8.33263(7)$ Å. This means the lattice parameter of NiFe$_2$O$_4$ can be determined with an accuracy up to 5 digits beyond the decimal point. Whereas in previous studies with X-ray diffraction [7], the accuracy of lattice parameter was only three digits after the decimal point, namely $a = 8.345$ Å. This is possible because neutrons interact with the nucleus of the atom, while X-ray interacts with the electrons of the atom. Neutron diffraction brings information about the position of the nucleus. While the X-ray difffraction data provides information on the position of the atom. The width of the electron cloud and the size of nucleus are around 1 Å, and 10^{-5}Å, respectively. Thus, the position of atoms will have much uncertainty. Therefore, information obtained from the neutron diffraction data is more accurate. The results of the present study are in accordance with the results of previous studies which were also carried out using the neutron diffraction technique, where the lattice parameter, $a = 8.3311(8)$ Å [11]. The coordinate fraction of the oxygen atoms in this work is $x_j = y_j = z_j = 0.2556(3)$ in accordance with the results of previous studies, namely $x_j = y_j = z_j = 0.2536(4)$ which was also obtained by neutron diffraction techniques [8].

The occupation factor of Fe^{3+} and Ni^{2+} cations both in A-site and B-site could be accurately determined with accuracy of up to three positions after the decimal points, and it was revealed that 14.6% of the A-site and 13.2% of the B-site were empty, both the A-site and the B-site were predominantly occupied by Fe^{3+} cations. The occupation factors of the Ni^{2+} in B-site is three times the occupation factors of Ni^{2+} in A-site, and the magnetic moment of A-site and B-site are 4.2(3) μ_B and 1.8(4) μ_B, respectively. Cations distribution among the A-site and B-site of NiFe$_2$O$_4$ is [Ni$_{0.002}$Fe$_{0.852}$][Ni$_{0.006}$Fe$_{0.862}$]$_2$O$_4$. The structure of NiFe$_2$O$_4$ deviated from an inverse spinel structure to a mixed spinel structure due to this cations redistribution or change in the coordination of the tetrahedral and octahedral sites. This deviation from the basic inverse spinel structure resulted in large magnetocrystalline anisotropy [12]. The Ni^{2+} and Fe^{3+} cations are aligned ferromagnetically in tetrahedral and octahedral lattices while are coupled antiferromagnetically between tetrahedral and octahedral sites [7]. Thus, the magnetic moment of NiFe$_2$O$_4$/formula unit (f.u) is $\mu = 2.4(5)$ μ_B.

The octahedral (B-site) sublattice is occupied by Fe^{3+} cations with 5 unpaired electrons in the 3d shell and Ni^{2+} cations with 2 unpaired electrons, resulting in a net

Table 2. **The Rietveld Refinement Results of Atomic Co-ordinate Fractions (x_j, y_j, z_j), and Occupation Factors (g_j), Lattice Parameters (a, b, c), Magnetic Moments (μ_A, μ_B), Weight Percent (W_t), and Average Crystallite Size (D_{av}) of NFO, 0.6NFO/0.4BTO and BTO**

Parameter		NFO	0.6NFO/0.4BTO
		$NiFe_2O_4$	$NiFe_2O_4$
Space group		*F d -3 m*	*F d -3 m*
V [Å^3]		578.558(8)	578.838(8)
$a = b = c$ [Å]		8.33263(7)	8.33398(6)
Fe1(8a):	x_j	0.125	0.125
	y_j	0.125	0.125
	z_j	0.125	0.125
	g_j	0.852(9)	0.8975(7)
Ni1(8a):	x_j	0.125	0.125
	y_j	0.125	0.125
	z_j	0.125	0.125
	g_j	0.002(8)	0.0250(7)
Fe2(16d):	x_j	0.5	0.5
	y_j	0.5	0.5
	z_j	0.5	0.5
	g_j	0.862(1)	0.950(1)
Ni2(16d):	x_j	0.5	0.5
	y_j	0.5	0.5
	z_j	0.5	0.5
	g_j	0.006(1)	0.012(1)
O(32e):	x_j	0.2556(3)	0.2554(3)
	y_j	0.2556(3)	0.2554(3)
	z_j	0.2556(3)	0.2554(3)
	g_j	1.0	1.0
μ_A [μ_B]		4.2(3)	4.5(4)
μ_B [μ_B]		1.8(4)	2.1(5)
W_t [%]		100	61.60(2)
D_{av} [nm]		118	76

Parameter		BTO	0.6NFO/0.4BTO
		$BaTiO_3$	$BaTiO_3$
Space group		*P 4 m m*	*P 4 m m*
V [Å]		64.100(5)	64.374(6)
$a = b$ [Å]		3.9924(1)	4.0130(1)
c [Å]		4.0213(2)	3.9972(3)
Ba(1a):	x_j	0.0	0.0
	y_j	0.0	0.0
	z_j	0.0	0.0
	g_j	0.8(5)	1.0
Ti(1b):	x_j	0.5	0.5
	y_j	0.5	0.5
	z_j	0.50(1)	0.44(3)
	g_j	0.8(5)	1.0
O1(1b):	x_j	0.5	0.5
	y_j	0.5	0.5
	z_j	0.028(6)	-0.01(2)
	g_j	0.8(4)	1.0
O2(1b):	x_j	0.5	0.5
	y_j	0.0	0.0
	z_j	0.523(6)	0.46(2)
	g_j	0.8(5)	1.0
W_t [%]		100	38.40(1)
D_{av} [nm]		57	89

magnetic of 7 μ_B/f.u. For the bulk $NiFe_2O_4$ spinel structure, the tetrahedral (A-site) sublattice which is only occupied by Fe^{3+} cations accounts with 5 μ_B/f.u. Thus, both sublattices do not compensate each other completely resulting in a net magnetic moment of 2 μ_B/f.u [13]. So, due to the mix spinel structure, then the magnetic moment of bulk $NiFe_2O_4$ increases to 2.4(5) μ_B.

Analysis of neutron diffraction data of the BTO sample is done using the one phase-input parameters, namely the $BaTiO_3$ nuclear phase. The results of the Rietveld profile fitting is shown in Figure 4, with the GOF of χ^2 = 1.6. As shown in Figure 4 that all of diffraction peaks measurement results coincide with the nuclear peaks calculation result. No impurity phases are observed within the detected limits of high resolution neutron diffraction.

Analysis of neutron diffraction data of the 0.6NFO/ 0.4BTO sample is carried using the three-phase input parameters, namely the nuclear phase and the $NiFe_2O_4$ magnetic phase parameters, and also the $BaTiO_3$ nuclear phase parameters. Similar to the case of the (NFO)$_M$ above, the Rietveld refinement is also done by trial and error method. First, the cations of Ni^{2+} are set to occupy the A-site predominantly. In the second case, the A-site is overwhelmingly occupied by the cations of Fe^{3+}. The Rietveld refinement based on the first and second assumptions gives a χ^2 value of 3.8 and 2.0, respectively. So, the second assumption is the most appropriate arrangement or setting, and the diffraction pattern of the analysis based on the second assumption is shown in Figure 5.

The upper-, the second-, and the third short vertical lines show the Bragg positions for the NFO nuclear phase, the NFO magnetic phase, and the BTO nuclear
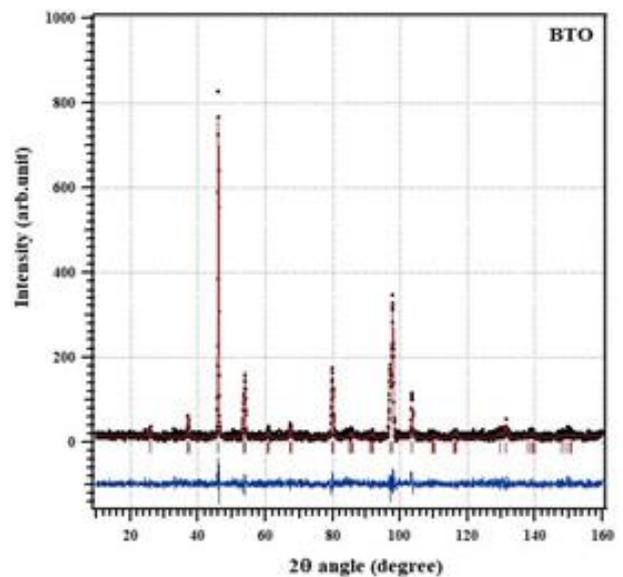

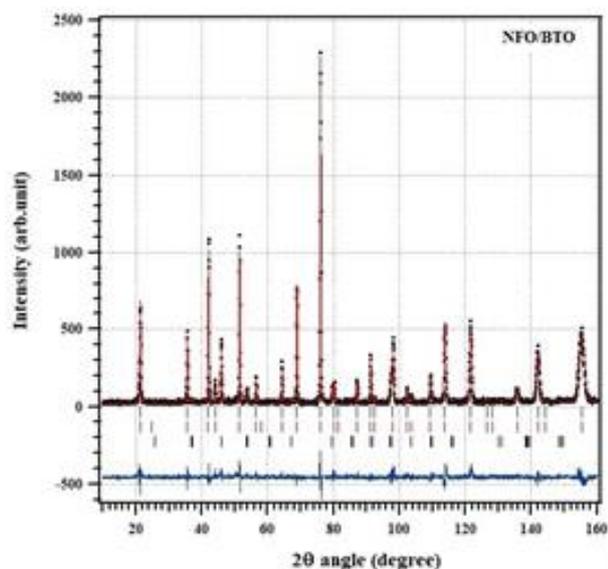**Figure 4. HRPD Neutron Diffraction Intensity Pattern of the BaTiO$_3$ (BTO) Sample**

Figure 5. HRPD Neutron Diffraction Intensity Pattern of the 0.6NFO/0.4BTO Sample

phase, respectively. The neutron diffraction patterns of the 0.6NFO/0.4BTO sample shows sharp peaks. No impurity phases are observed within the detected limits of high resolution neutron diffraction. The Rietveld refinement results of atomic coordinate fractions (x_j, y_j, z_j), and occupation factors (g_j), lattice parameters (a, b, c), magnetic moments (μ_A, μ_B), weight percents (W_t), and average crystallite size (D_{av}) are shown in Table 2.

The occupation factor of Fe^{3+} and Ni^{2+} cations both in A-site and B-site could be accurately determined with accuracy of up to three positions after the decimal points, and it was revealed that 7.75 % of the A-site and 3.80 % of the B-site were empty, both the A-site and the B-site were predominantly occupied by Fe^{3+} cations, and occupation factors of Ni^{2+} in A-site is two times the occupation factors of Ni^{2+} in the B-site, the magnetic moment of the A-site and B-site are 4.5(4) μ_B and 2.1(5) μ_B, respectively. Thus, the magnetic moment of $NiFe_2O_4$/f.u is $\mu = 2.4(5)$ μ_B. Cations distribution among the A-site and B-site of $NiFe_2O_4$ is $[Ni_{0.0250}Fe_{0.8975}]$ $[Ni_{0.012}Fe_{0.950}]_2O_4$.

$BaTiO_3$ has a tetragonal unit cell with lattice parameters, $a = b = 3.9924(1)$ Å, $c = 4.0213(2)$ Å, in accordance with previous work, where $a = b = 3.997$ Å, $c = 4.031$ Å [14]. $NiFe_2O_4$ is the cubic spinel with lattice constant, $a = 8.33263(7)$ Å, as mentioned earlier, this is also consistent with the results of previous studies [11], $a = 8.3311(8)$ Å. This lattice parameter of $NiFe_2O_4$ increases from 8.33263(7) Å to 8.33398(6) Å and the $NiFe_2O_4$ unit cell volume increases from 578,558(8) Å³ to 578,838(8) Å³. Similarly, the a and b lattice parameters of BTO increase from 3.9924(1) Å, to 4.0130(1) Å, but the c lattice parameter of BTO

decreases from 4.0213(2) Å to 3.9972(3) Å on composite. Thus, the BTO content in the composite has caused tensile strains induced into the NFO lattice, and at the same time, the tensile strains of NFO caused the compressive strain on the BTO even though the unit cell volume of BTO is also increasing from 64.100(5) to 64.374(6) Å³.

Due to the presence of BTO in NFO/BTO composite, Ni^{2+} cations move from B-site to A-site. Initially the amount of Ni^{2+} at A-site was one-third of Ni^{2+} cations on B-site, because the presence of BTO has undergone a reversal the number of Ni^{2+} on the A-site was twice as much as Ni^{2+} cations on the B-site. According to [7] the reason for the displacement of Ni^{2+} cations is that the O^{2-} ions can be easily removed from the B-site position rather than the A-site due to the weak coupling in the B-site position. Therefore the role of BTO as the driving force behind the movement of part of the Ni^{2+} cations from the B-sites to the A-sites has been confirmed.

The plot of the magnetization curve, M versus the magnetic field, H from the NFO and 0.6NFO/0.4BTO composite samples is shown in Figure 6. The zoomed middle part of the hysteresis loops from samples of NFO and NFO/BTO is indicated in Figure 7. In Table 3 it is shown that the saturation magnetization at room temperature, M_s of $NiFe_2O_4$ decreases from 49.4 to 35.9 emu/g in the 0.6NFO/0.4BTO composite. This is a logical consequence because M_s is measured per unit volume (weight) of the sample. The smaller the volume of magnetic material, the less the number of magnetic domains that will accumulate to produce a magnetic moment/unit volume.
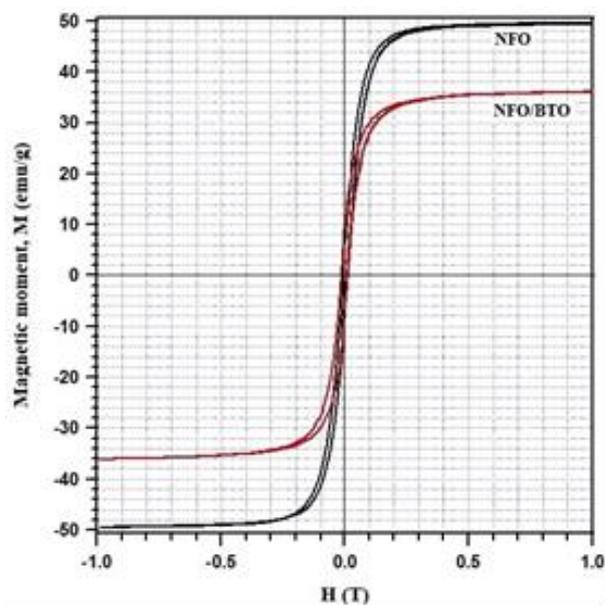

Figure 6. The Magnetization Curve, *M* versus the Magnetic Field, *H* of the NFO/BTO and NFO Samples
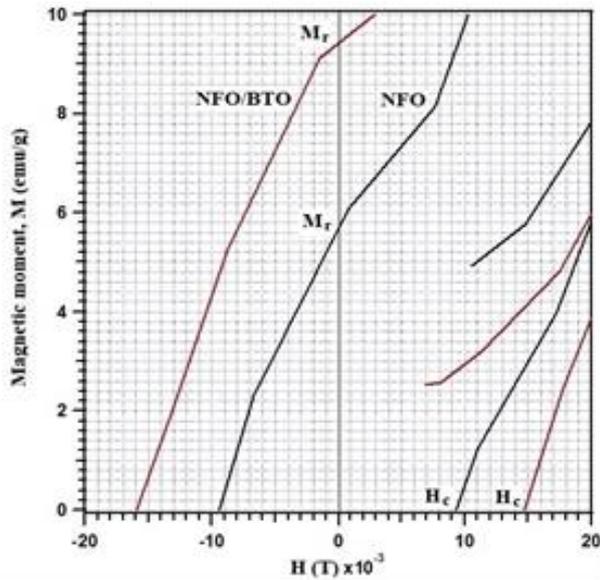
Figure 7. Zoomed Middle Part of the Hysteresis Loops from Samples of NFO and NFO/BTO

Table 3. Magnetic Properties of the NFO/BTO, and NFO Composites

Sample	Magnetic parameters		
	M_s (emu/g)	M_r (emu/g)	H_c (Oe)
NFO	49.4	5.6	93
NFO/BTO	35.9	9.4	147

The coercive field, H_c of NFO and 0.6NFO/0.4BTO composite are 93 and 147 Oe, respectively. This is possible so if this composite is nanocrystalline material. The crystallite size, D of the sample was calculated from each of the reflections in the neutron diffraction pattern using the formula, $D = k\lambda/\beta cos\theta$, where λ, β, and θ are the wavelengths of the neutron beam, full width at half maximum, and Bragg peak position, respectively [15]. The calculated-crystallite sizes are shown in Table 2. The crystallite size of NFO, BTO and 0.6NFO/0.4BTO are 118, 57 and 76 nm, respectively. The 0.6NFO/0.4BTO composite, and BTO are nanocrystalline material, because it have a crystallite size smaller than 100 nm suggesting a superparamagnetic behaviour for the nanocrystalline of 0.6NFO/0.4BTO composite. In addition, a low coercive field, H_c render the composite more suitable for use as soft magnetic material [16]. Why for NFO with 118 nm paticle size, but H_c is lower than H_c from 0.6NFO/0.4BTO composite with 76 nm particle size. This case can be attributed to the reduction of domain wall energy caused by the weak magneto-crystalline anisotropy [17].

4. Conclusions

Neutron diffraction study on the 0.6NFO/0.4(BTO) multiferroic composite has been carried out. The 0.6NFO/0.4BTO multiferroic composites together with NFO, and BTO samples have been synthesized by solid reaction method using high energy milling. Rietveld refinement of the neutron diffraction data was performed to deduce the basic structural parameters, and cations distribution of NFO. The cations arrangement was obtained by refining the occupancy of individual cations at tetrahedral and octahedral sites. Both NFO and 0.6NFO/0.4BTO samples have a mixed spinel structure. The effect of adding BTO as a composite is to increase Ni^{2+} cations occupancy on A-site. The magnetic moment of multiferroic 0.6NFO/0.4BTO composite and NFO is of the same value of $\mu = 2.4(5)$ μ_B. The BTO content in the composite has caused tensile strains induced into the NFO lattice, and at the same time, tensile strains of NFO caused the compressive strain on the *c* lattice of BTO even though the unit cell volume of BTO is also increasing.

Acknowledgements

References

[1] W. Eerenstein, N.D. Mathur, J.F. Scott, Nat. 442 (2006) 759.
[2] J. Zhai, M. Peng, M. Song, L. Yudong, Recent Prog. Magn. Multiferroic Mater. (2014) 25.
[3] Y. Shen, Mater. Sci. Eng. (2014) p.1.
[4] W-G. Yang, Mater. Sci. Eng. (2016) p.1.
[5] V. Sharma, P. Rani, B.K. Kunar, Adv. Mater. Proc. 1(1) (2016) 65.
[6] X. Yang, Elec. Eng. (2013) p.52.
[7] B. Sarkar, B. Dalal, V.D. Ashok, K. Chakrabarti, A. Mitra, S.K. De, J. Appl. Phys. 115 (2014) 123908.
[8] A.P. Nosov, M.A. Semkin, A.E. Teplykh, S.G. Bogdanov, N.V. Urusova, Y.N. Skryabin, A.N. Pi-rogov, V.G. Vasiliev, E.V. Vladimirova, T.S. Kar-pova, Solid State Phenom. 233-234 (2015) 371.
[9] N.G.G. Imam, Solids State Phys. (Mater. Sci.), 2013, p.1
[10] J. Rodriguez-Carvajal, France, 2015, p. 11.
[11] Anonymous, N. Ferrite, Nanosyst. 2018, p.69. http://shodhganga.inflibnet.ac.in/bitstream/10603/2 5791/11/11_chapter%202.pdf.

[12] M. Yehia, S.M. Ismail, S.S. Ata-Allah, Sh. Labib, M.B. Mohamed, Mag. Nanostructured Mater. 11 (2018) 323.

[13] M. Hoppe, Key Technol. 118 (2016) p. 10.

[14] A. Mahmoud, A. Erba, Kh. E. El-Kelany, M. R´erat, R. Orlando, Phys. Rev. B. 89, (2014) 045103(1).

[15] S. Ryufuku, Y. Tomota, Y.Shiota, T. Shiratori, H. Suzuki, A. Moriai, Mater. Sci. Forum. 539-543 (2007) 2281.

[16] M.A.F. Ramalho, A.C.F.M. Costa, L. Gama, R.H.G.A. Kiminami, E.P. Hernandez, D.R. Cornejo, S.M. Rezende, https://www.ipen.br/ biblioteca/cd/pt ech/2005/PDF/21_06.PDF.

[17] M.B. Ali, K. El-Maalam, H. El-Moussaoui, O. Mounkachi, M. Hamedoun, R. Masrour, E.K. Hlil, A. Benyoussef, J. Magn. Magn. Mater. 398 (2016) 20.